Quantitative proteomic analysis of beef tenderness of Piemontese young bulls by SWATH-MS

María López-Pedrouso[1], José M. Lorenzo[2,3], Liliana Di Stasio[4], Alberto Brugiapaglia[4] and Daniel Franco[2]*

[1]Department of Zoology, Genetics and Physical Anthropology, University of Santiago de Compostela, Santiago de Compostela, 15872, Spain

[2]Centro Tecnológico de la Carne de Galicia, Rúa Galicia Nº 4, Parque Tecnológico de Galicia, San Cibrao das Viñas, Ourense, 32900, Spain

[3]Área de Tecnología de los Alimentos, Facultad de Ciencias de Ourense, Universidad de Vigo, 32004 Ourense, Spain

[4]Department of Agricultural, Forest and Food Sciences, University of Turin, Largo Braccini 2, 10095 Grugliasco, Torino, Italy

*corresponding author: danielfranco@ceteca.net;

Abstract

Meat consumer satisfaction is largely defined by meat tenderness. However, it is a complex trait which mainly depends on structural and metabolic proteins. Quantitative proteomic approach is a suitable way to tackle the tenderness. Ten aged-beef samples from Piemontese breed classified as tender and tough meat were evaluated using SWATH-MS and bioinformatic tools for revealing the main biochemical events. Between the two textural groups, proteomic changes were mainly caused by 43 differentially abundant proteins (DPAs) arranged in reference patterns as displayed the heat map analysis. Most of these DPAs were associated with energy metabolism. From the functional proteomic analysis, two clusters of proteins, including ACO2, MDH1, MDH2 and CS in one cluster and FBP2, PFKL, LDHA, TPI1 and GAPDH/S in the other cluster, suggest gluconeogenesis, glycolysis and citrate cycle as key pathways for beef tenderness. These findings contribute to a deeper insight into molecular pathways related to beef tenderness.

Keywords: cattle, tenderization, mass spectrometry, glycolysis and citrate cycle, gene ontology

1. Introduction

Tenderness, juiciness and flavour are the most distinctive characteristics of beef-eating experience. If any of these three traits is not fulfilled, it would be detrimental to overall palatability, decreasing the level of meat quality (Henchion et al., 2017; O'Quinn et al., 2018). The lack of tenderness could result in considerable economic losses, reducing consumer confidence. Regarding beef tenderness, in recent years substantial efforts have been undertaken in the field. Special emphasis is being constantly upgraded in the improvements of production, pre-slaughter and processing factors (Bhat et al., 2018; Mwangi et al., 2019; Picard & Gagaoua, 2017). Additionally, it has been highlighted that tenderness instrumental differences not always lead to differences in the product sensory profile, because of the complexity of this in meat heterogeneous product. Therefore, a noticeable improvement of beef tenderness is needed to positively influence the consumer´s perception (López-Pedrouso et al., 2020). It is necessary to have more control on the ultimate pH, the cathepsin and calpain/calpastatin activity, proteasome, collagen content and heat shock proteins among other factors, as well as a deeper knowledge of the molecular mechanisms behind the meat tenderness to understand completely the whole process (Zapata et al., 2009). In the process of muscle-to-meat conversion, preliminary biochemical modifications are involved starting from the vital functions stops (Lana & Zolla, 2016). During beef ageing, structural changes of the myofibril units associated with myofibrillar proteolysis, intermediate filaments releasing, actin and myosin breaking as well as cytoskeletal proteins and the calpain system are related to tenderness (Anderson et al., 2012). Consequently,

myofibrillar and sarcoplasmic proteins play a key role in this cascade of events contributing to final tenderness and proteomic analysis is particularly relevant.

The past decade has seen the rapid development in proteomic technologies enabling the identification and quantification of overall proteins in a cell, tissue or organism more accurately and precisely. Indeed, recent developments of the meat tenderness study from a proteomic point of view have been published (Carlson et al., 2017; López-Pedrouso et al., 2019; Picard & Gagaoua, 2017). Progress in the quantitative proteomic field, as well as in other OMICs technologies (genomics, transcriptomics) and bioinformatics (Picard & Gagaoua, 2020), also offers powerful data of the molecular mechanisms behind beef tenderness. Particularly, label-free proteomics has been used as a tool for the identification of protein biomarkers in beef tenderness (Boudon et al., 2020). Most recently, SWATH-MS (sequential window acquisition of all theoretical mass spectra) arises as a result of an improvement in mass spectrometry-based proteomics techniques using data-independent acquisition (DIA) method. First of all, protein samples are digested by trypsin and the resulting peptides are separated and identified using liquid chromatography followed by tandem mass spectrometer using a DDA (Data-dependent acquisition) method to generate a reference spectral library. The strategy "peptide query parameters", based on peptide-centric scoring using the querying data of chromatographic and mass spectrometric parameters for the resulting proteins and peptides, has been developed. Afterwards, the quantification of proteins by DIA-based SWATH-MS has proven to achieve excellent reproducibility (Anjo et al., 2017; Ludwig et al., 2018). In bovine muscle proteome, a comparison between selected reaction monitoring (SRM) and SWATH methods was done and it has been demonstrated

that SWATH-MS is more efficient and suitable for a larger panel of proteins with a robust quantification (Wu et al., 2019).

Piemontese is a breed characterized by muscular hypertrophy as a result of the guanine-to-adenine transition at position 938 in exon 3of myostatin gene. This breed is homozygous for this missense mutation that results in an inactive myostatin form (Boukha et al., 2011). Carcass and meat quality traits have been studied previously (Pegolo et al., 2020; Savoia et al., 2019). The main impact of this genotype is appreciated in muscle mass development, as double muscling improving the meat yield (O'Rourke et al., 2013). Moreover, this mutation leads to lower fat content and marbling, but a higher number of muscle fibres (type II). This genotype prevents the proteolytic process, but tenderness is increased by the higher number of muscle fibres and decreased collagen content (Chen & Lee, 2016). For these reasons, the Piemontese breed was used in this study on tenderness molecular mechanisms.

The aim of this study was to investigate the molecular mechanisms which regulate the meat tenderness in *Longissimus thoracis* of Piemontese cattle as well as to search the protein biomarkers linked to tenderness for potential biotechnological application in the meat industry.

2. Materials and methods

2.1. Animal sampling selection

The present study is part of the "Qualipiem" project, which was aimed at exploring the possibility of improving the meat quality traits in Piemontese cattle using innovative selection strategies. The research involved 1327 young bulls from 115 farms operating six different beef farming systems. The young bulls were all

enrolled in the Herd Book of the Italian Piemontese breed, were sired by artificial insemination bulls, and were reared on commercial farms representative of the farming systems in the Piemonte region (NW Italy). The characteristics of the beef systems, feeding practices, and animal slaughter are described in detail by Savoia et al. (2019)

Briefly, all animals were slaughtered at the same commercial EU-licensed slaughterhouse from April 2015 to February 2017. The average age at slaughter was about 17 months (508±58d), the average carcass weight was 414 ±36 kg, and 66.7% of the carcasses had a muscularity grading of E (excellent) determined according to the SEUROP classification system (Commission of the European Communities, 1982).

Twenty-four hours after slaughter, a meat sample (from the fifth and sixth thoracic vertebrae) of *Longissimus thoracis* (LT) muscle was collected from the half right carcass of each animal, vacuum-packed and aged at 4°C for 7 days. After ageing, the samples were removed from their respective packaging, weighed to determine purge loss and divided into two slices (2.0 cm thick); one slice was used to measure pH and meat colour and to determine water content; the second one was used for cooking loss and shear force determination. Additionally, approximately 50 g of homogenised muscle were lyophilized, ground in a blender and stored at -80°C until intramuscular fat, protein, collagen content, collagen solubility and proteome analyses were performed.

For proteomic analysis, a subset of 10 freeze-dried meat samples, traceable to five farms, were selected “a posteriori” on the basis of Warner-Bratzler shear values, in order to form two groups of five samples each, classified as tender (< 30 N) and though (> 60 N). To minimize the effect of extrinsic pre-slaughtering

132 factors on meat tenderness, the selection was done so to have couple of samples
133 (one sample with low and one with high Warner Bratzler value) derived from
134 animals reared in the same farm and slaughtered on the same day.

135 As tenderness can be also influenced by the genotype at the *myostatin* locus, the
136 samples were analysed to make sure that all derived from animals homozygous
137 for the *mh* allele.

138 **2.2. Analysis of meat quality traits**

139 The ultimate pH measurements were taken with a spear-type electrode
140 connected to a Crison portable pH-meter (Crison Instruments, S.A., Alella,
141 Spain).

142 Meat colour was measured with a Minolta CR-331C Chroma Meter set with D65
143 illuminant and the 2° standard observer. Measurements were taken after 1 h of
144 blooming on a freshly cut surface of a 2.0 cm thick steak. Results were expressed
145 as lightness (L*), redness (a*) and yellowness (b*) values in the CIELAB colour
146 space model. The parameters Chroma (C*), related to the intensity of colour, and
147 hue angle (h*), related to the change of colour from red to yellow, were calculated
148 as follows: $C^* = (a^{*2} + b^{*2})^{0.5}$; $h^* = \tan^{-1} b^*/a^*$. In addition, the reflectance values
149 from 400 to 700 nm were acquired by a Minolta CM600d Spectrophotometer set
150 with specular component excluded, D65 illuminant and 10° standard observer.
151 Reflectance values at wavelengths not given by the instrument (474, 525 and 572
152 nm) were calculated using linear interpolation. The reflectance values were
153 converted to K/S ratios (absorption and scattering coefficients ratios) using the
154 following equation: $K/S = (1-R)^2 \div 2R$, where R represents the % reflectance
155 expressed as decimal. The ratios $K/S_{474} \div K/S_{525}$, $K/S_{572} \div K/S_{525}$ and $K/S_{610} \div K/S_{525}$

were used to estimate Deoxymyoglobin (DMb), Metmyoglobin (MMb) and Oxymyoglobin (OMb) percentage, respectively.

The moisture content of meat samples was determined by oven drying until constant weight at 125°C for 5h. The freeze-dried samples were used to analyse the crude fat, crude protein, collagen content and collagen solubility. The crude fat content was determined by petroleum ether extraction using a Soxhlet apparatus (Büchi Extraction System B-811; Flawil, Switzerland). The nitrogen content was determined by Kjeldahl method using a Büchi Distillation Unit K- 355 (Flawil, Switzerland), and a nitrogen-to-protein conversion factor of 6.25 was used to calculate the protein content. The crude fat and protein contents were then expressed as percentages of the raw meat.

Total collagen concentration and collagen solubility of meat samples were determined by measuring the hydroxyproline content in both the soluble and insoluble fractions. Prior to hydroxyproline determinations, the soluble and insoluble fractions were separated by centrifugation after heating in a water bath at 80°C for 2h. The spectrophotometric determination of hydroxyproline in both fractions was based on the oxidation of hydroxyproline by chloramine-T, followed by the addition of 4-dimethyl-aminobenzaldehyde, which generates a colored complex quantifiable spectrophotometrically at 558 nm. Total hydroxyproline content was calculated as the sum of soluble and insoluble fractions and soluble collagen was expressed as percentage of total hydroxyproline. Results were expressed as µg hydroxyproline/g fresh muscle. The conversion factor of 8 was used to transform the amount of hydroxyproline into collagen.

The water holding capacity (WHC) was measured as purge (PL) and cooking loss (CL) and expressed as a percentage. Purge losses were computed as the

difference between the weight of the packaged sample and the weight of the sample dried using blotting paper plus the weight of the heat dried bag, and was expressed as a percentage of the sample weight. For cooking losses determination, the slices were weighed, sealed in a polyethylene bag and cooked in a water bath, set at 75 °C until reaching an internal core temperature of 70°C monitored with a thermocouple. After cooking, the slices were cooled under cold water, while still in bags. Then the slices were removed from the bags, blotted and reweight. Cooking losses were computed as the amount of weight lost after cooking, expressed as a percentage of the weight of the uncooked slice.

After cooking loss determination, the slices were wrapped in a plastic film, stored in a cooler at 4°C overnight and then used for Warner Bratzler shear force (WBSF) analysis. At least six 1.27 cm diameter cores, approximately 2 cm long of cooked meat from each slice, were removed parallel to the longitudinal orientation of the muscle fibres and sheared perpendicular to the muscle fibres orientation using an Instron Universal Testing Machine (Model 5543, Instron Corp., USA) equipped with a Warner-Bratzler shear device (100-kg load cell and crosshead speed of 200 mm/min). The maximum WBSF (N) recorded during analysis indicated by the highest point in the curve shear force-time was determined. Warner-Bratzler slope was calculated to express shear firmness (SF; N/s) as the slope of the line drawn from the origin of the curve to the maximum peak force with higher values corresponding to lower elasticity. Total energy (TE; N x mm) corresponding to the total area under the WBSF curve, was used to describe the total energy consumed to chew the meat until it could be swallowed.

2.3. Proteomic analysis

2.3.1. Extraction and digestion of proteins

Fifty mg of lyophilized meat were homogenised in RIPA buffer consisting of 200 mmol/L Tris/HCl (pH 7.4), 130 mmol/L NaCl, 10% (*v*/v) glycerol, 0.1% (v/v) SDS, 1% (v/v) Triton X-100, 10 mmol/L $MgCl_2$ with anti-proteases and anti-phosphatases (Sigma-Aldrich, St. Louis, MO, USA) using a TissueLyser II (Qiagen, Tokyo, Japan). The resulting solution was centrifuged at 14,000*g* at 4 °C for 20 min and the quantification of protein was assessed by RC-DC kit (Biorad Lab., Hercules, CA, USA). To clean the sample, 100 µg were loaded on an SDS-PAGE (10%) and concentrated the proteins in a single band. The gel band was cut into pieces and washed by Milli-Q water followed by 50 mM ammonium bicarbonate in 50% methanol. Then, the pieces were dehydrated by acetonitrile in a vacuum centrifuge. The reduction of proteins was carried out with 10 mM DTT in 50 mM ammonium bicarbonate at 60 °C for 30 min and the alkylation with 55 mM iodoacetamide in 50 mM ammonium bicarbonate at room temperature for 30 min in darkness. Finally, the proteins were digested with 20 ng/µL trypsin (Promega, Madison, USA) in 20 mM ammonium bicarbonate incubating at 37 °C for 16 h. This resulting solution was diluted in 0.1% formic acid for further analysis.

2.3.2. Generation of the reference spectral library by DDA acquisition

A sample representative of each group was obtained mixing 4 µg of protein from each sample and they were analysed by shotgun data-dependent acquisition (DDA) approach by micro-LC-MS/MS. The liquid chromatography was carried out by micro-LC system Ekspert nLC425 (Eksigen, Dublin, CA, USA) using an YCM-TriartC18 column (150 µm × 0.3 mm, 12 nm, s-3 µm) (YMC CO, Japan) running at a flow rate of 5 µL/min. A 40 min gradient from 95% B (0.1% formic acid in acetonitrile) and 5% A (0.1% formic acid in water) to 5% Buffer B. The mass

spectrometer was a hybrid quadrupole-TOF mass spectrometer, model Triple TOF 6600 (SCIEX, Framingham, MA, USA) operating with data-dependent acquisition system in positive ion mode. The mass range was from 100 to 1500 m/z with an accumulation time of 0.25 s for a total cycle time of 2.8 s. To create the library, the MS raw files and databases searches were combined and performed using ProteinPilot software v.5.0.1. (SCIEX, Framingham, MA, USA). The searches were conducted through Uniprot Swiss-Prot database for *Bos taurus (Bovine)*

2.3.3. Quantification of proteins by DIA acquisition

The SWATH-MS acquisition was performed in a DIA mode with two technical replicates in each meat sample and five biological samples in each meat group. A sample of proteins (4 µg) was subjected to each determination. The MS/MS analysis was carried out in a cyclic manner using an acquisition time of 50 ms in a total cycle time of 6.3 s. A cycle of SWATH consisted of 65 scans in a mass range of 400 to 1250 m/z and a variable width of 1 m/z overlap. The spectral alignment and targeted data extraction were performed by PeakView v.2.2. (SCIEX, Framingham, MA, USA). All DIA files were loaded using the following settings: ten peptides/protein and seven fragments/peptide, excluded shared and modified peptides and FDR below 1%. The quantification of proteins was measured by the peak area of the given peptides using *p*-value scoring of 0.05 and a fold change of 1.5 as the cut-off. Finally, the proteins with differentially abundance were identified using Student's *t*-test.

2.4. Statistical analysis

Data from meat quality for the two textural groups were submitted to one-way ANOVA analysis. Previously, normal distribution and variance homogeneity were tested (Shapiro-Wilk). Statistical analysis was carried out using the SPSS package (SPSS 23.0, Chicago, IL, USA). The least squares mean (LSM) were separated using a Duncan *t*-test. All statistical tests of LSM were performed for a significance level $P<0.05$. The standard error of the mean (SEM) was obtained as the standard deviation (SD) divided by the square root of the sample size.

For proteomic analysis to assess statistical differences among proteins, a Student's *t*-test was done at a level of confidence of 95%. The correlations among individual protein quantifications and textural meat parameters were determined by Pearson's linear correlation coefficient at two levels ($P < 0.01$ and $P < 0.05$).

For bioinformatic and multivariate analysis, hierarchical clustering of the identified proteins by SWATH-MS was generated by XLSTAT 2.01 (Addinsoft SARL, Paris, France) based on the protein quantifications by mean of the heat map, using Euclidean distances. The differentially abundant proteins were studied by heat map analysis using the logarithms of protein quantification for each biological replicate. To understand the cellular processes, Gene Ontology (GO) enrichment and protein-protein interaction (PPI) were carried out using STRING 10.0. (Search Tool for the Retrieval of Interacting Genes/proteins).

3. Results and discussion

3.1. Characterization of tender and tough meats

The determination of meat quality parameters allowed us to assess the suitable biological material to unravel proteome changes related to tenderness during the transformation of bovine muscle into the meat. Table 1 shows mean values of

chemical composition, colour measurements, water holding capacity and textural parameters. The samples were chosen to ensure that statistically significant differences by the one-way Anova (P<0.05) were only detected in textural parameters. Indeed, it can be observed that the other parameters were not statistically different. The Piemontese breed is highly specialized for beef production due to double-muscle phenotype, which depends on a specific mutation in *myostatin* gene (mh). The syndrome has been associated with superior carcass characteristics and meat quality traits compared to normal animals. Indeed, the dressing yield is about 5% higher than in non-double muscled animals at similar age or weight and the carcasses have a larger proportion of expensive cuts and a lower proportion of fat and bone than normal animals (Biagini & Lazzaroni, 2005). In the present study, carcass weight ranged from 408.4 to 418.8 kg (P=0.678) at the age of 503.6 to 511.8 days (P=0.839) in the tender and tough groups, respectively.

Regarding the chemical composition, there were no significant differences between groups for any trait. High values of protein were found with an average percentage greater than 22.60% in both groups, meanwhile, intramuscular fat percentages varied between 0.92% and 1.15%, indicating the characteristic leaner muscle for this breed. The Piemontese meat has a high value due to its low intramuscular fat content and high tenderness. In relation to meat composition, the hypertrophied Piemontese breed compared to other breeds (e.g. Limousin and Friesian breeds) has higher water and protein content and, because of the lower collagen content, protein quality in terms of essential amino acids content is improved. The meat is also characterized by low intramuscular fat content (1% or lower) and relatively high PUFA content because of the greater

303 proportion of membrane phospholipids versus triacylglycerol. The high ratio of
304 phospholipids to triacylglycerols contributes to the high PUFA/SFA ratio
305 (Brugiapaglia et al., 2014).

306 Meat colour largely depends on the amount of myoglobin and its oxidation state.
307 In the absence of oxygen, the myoglobin produces a purple-red colour. However,
308 the myoglobin reacts with oxygen resulting in oxymyoglobin. The colour produced
309 by oxymyoglobin is bright red very appreciated by consumers. In the case of long
310 storage time, the colour turns into brown colour due to the transformation of
311 oxymyoglobin into metmyoglobin. Over time, the meat becomes tenderer, but the
312 colour could darken too much for consumers. In the case of Piemontese, this
313 breed has a lower myoglobin concentration and lighter muscle colour than normal
314 animals and shows a lower water holding capacity estimated as drip/purge and
315 cooking losses probably due to the faster *post mortem* pH fall (Barge et al. 1996).
316 Additionally, previous studies have demonstrated that the ageing of Piemontese
317 meat should last over 7 days in order to improve quality parameters (Brugiapaglia
318 & Destefanis, 2011). As shown in Table 1, the Piemontese meat displayed high
319 values of lightness (38.06-39.96%) and redness (28.00-29.14%) resulting from
320 the fact that meat ageing was carried out in vacuum conditions

321 Regarding meat tenderness, literature concerning double-muscled cattle are
322 coherent on most but not all points. In fact, meat tenderness and tenderization
323 are complex phenomena determined by a number of factors. In general, muscles
324 of hypertrophied cattle have lower collagen (connective tissue) content which is
325 made up of a lower proportion of stable non-reducible cross-links, making the
326 meat more tender. Other factors, such as the smaller muscle fibres in double-
327 muscled animals, contribute to the increased tenderness in meat (Arthur, 1995).

In the present study, differences between both groups in collagen soluble fraction (P=0.002), shear force and firmness were highly significant (P<0.001).

3.2. Differential proteomic analysis of beef tenderness using SWATH-MS

To reveal the proteomic differences between tough and tender meat, SWATH-MS technology was used. In LT of Piemontese young bulls, an average of 261 proteins were detected and quantified using two technical replicates in each meat sample. To analyse major changes, the fold change higher than 1.5 and lower than 0.67 between textural groups was considered. As shown in Table 2, forty-three proteins were differentially abundant proteins (DAP) between the two textural groups (tough and tender meat). A set of 14 DAPs were more abundant in tough meat, whereas the remaining 29 DAPs were more abundant in tender meat, inferring strong proteomic changes linked to texture modifications. These proteins are proposed as biomarkers and only a further validation should be required. As extensively reviewed by (Gagaoua, Terlouw, et al., 2020b; Huang et al., 2020), some potential biomarkers of beef tenderness could be associated with muscle contraction, metabolism, heat stress, oxidation, proteolysis and apoptosis as shown in the present study.

A heat map analysis was carried out with these 43 DAPs using the protein quantification of each biological sample. Five biological samples for each textural group (tender and tough) were considered as displayed in Figure 1. It can be observed that the samples were separated into two clusters, the first cluster only contains tough meat, meanwhile, the second cluster includes tender meat. This suggests the existence of a proteomic pattern for tenderness meat in the case of LT in Piemontese breed. Additionally, this fact corroborates the idea that the

proteomic shifts were not random, indeed the reference pattern of proteins was strongly linked to tenderness.

Furthermore, these 43 DAPs were correlated with the textural parameters (shear force, firmness and energy) using Pearson's correlation analysis (Table 3). As expected, most of these proteins showed a clear association with Warner-Bratzler parameters, especially with WBSF (number of significant correlations with proteins and regression coefficient values), which is the most used trait for assessing the meat tenderness. The highly correlated proteins were heat shock cognate 71 kDa protein (HSPA8), glyceraldehyde-3-phosphate dehydrogenase (GAPDH), s-formylglutathione hydrolase (ESD), fructose-1,6-bisphosphatase isozyme 2 (FBP2), rab GDP dissociation inhibitor (GDI2), malate dehydrogenase (MDH1), triosephosphate isomerase (TPI1), glycerol-3-phosphate dehydrogenase (GPD1), protein-L-isoaspartate O-methyltransferase (PCMT1), striated muscle enriched protein kinase (SPEG), citrate synthase (CS), dipeptidyl peptidase 3 (DPP3) and peroxiredoxin 1 (PRDX1). Thus, these proteins may be proposed as protein biomarkers in LT of Piemontese cattle in relation to meat tenderness.

Regarding biological function, most proteins have a catalytic activity except for GDI2. It should be noted that myofibrillar proteins were not affected by variation in tenderness shown in the two groups in contrast to other studies (Anderson et al., 2012; Marino et al., 2013; Moczkowska et al., 2017). During *post-mortem* tenderization, the major cytoskeletal structures are degraded, affecting not only tenderness but colour and pH decline. Indeed, meat colour variation is largely due to shrinkage of myofilaments, myofibrils and muscles fibres affecting achromatic light scattering properties (Hughes et al., 2020). On the other hand, it

has been demonstrated that higher pH provokes an electrostatic repulsion between myofibrillar proteins contributing to a less lateral shrinkage of muscle fibres (Pearce et al., 2011). These two facts demonstrated the connection between the degradation of muscle fibres and tenderness or colour. However, the meat samples chosen for this study did not show differences in pH and meat colour (Table 1). Consequently, it would be appropriate to propose that no differences in structural degradation were found between the two groups. Nevertheless, most DPAs were associated with catalytic activities. Enzymatic reactions involved in the glycolysis and tricarboxylic acid cycle pathway are generally associated with energy metabolism in early *post-mortem* because of an anoxia situation (Jia et al., 2007). In the conditions of the present study, our findings suggest that beef tenderness of Piemontese breed could be produced by differences in energy metabolism during early *post-mortem*.

3.3. Functional proteomic analysis of beef tenderness

Functional proteomic and biochemical analysis let us reveal the crucial biological pathways behind tenderness in beef. As mentioned above, bovine meat between two textural groups showed meaningful differences on the proteome and 43 DAPs were proposed as biomarkers in the LT muscle of Piemontese. These proteins were also used in gene enrichment analysis (FunRich) within the category of the biological process shown in Figure 2A. The individual GO terms were ordered according to its p-value (red). Additionally, the percentage of genes included in each biological process (blue) and the reference value (green) are depicted. The most relevant GO terms were “glycolytic process” (P<0.001), “gluconeogenesis” (P<0.001) and “carbohydrate metabolic process” (P<0.001). It should be noted that carbohydrate metabolism includes both glycolysis and

gluconeogenesis as metabolic processes of glucose degradation or synthesis, respectively. In this sense, the glycolysis process and gluconeogenesis seem to be the most relevant pathways involved in the meat tenderization process. In accordance with other authors, enzymes associated with glycolysis and Krebs cycles were previously proposed as biomarkers of tenderness as well as proteins against oxidative stress (Ouali et al., 2013). Changes in proteins of different metabolic pathways were observed affecting meat tenderness. Our results match those observed in recent studies (Antonelo et al., 2020; Gagaoua, Terlouw, et al., 2020b; Malheiros et al., 2019).

STRING analysis was carried out to study a proteome-scale interaction network using published literature, experimental interactions of proteins and genomic data (Figure 2B). The resulting network is composed of 38 nodes (proteins) and 45 edges (interactions) (threshold: 0.7; high confidence). There were 14 proteins without interactions with other proteins, but the large majority of proteins displayed interactions. The p-value of PPI enrichment was lower than $1 * 10^{-16}$ and the local clustering coefficient was 0.511 indicating that 24 proteins were strongly connected as a group. Regarding biological processes, two clusters were displayed with proteins more strongly linked. One cluster comprised of aconitate hydratase (ACO2), malate dehydrogenase (MDH1, MDH2) and citrate synthase (CS). The other cluster includes fructose-1,6-bisphosphatase isozyme 2 (FBP2), ATP-dependent 6-phosphofructokinase (PFKL), L-lactate dehydrogenase (LDHA), glucose-6-phosphate isomerase (GPI), triosephosphate isomerase (TPI1) and glyceraldehyde-3-phosphate dehydrogenase (GAPDH/S). Indeed, these two clusters are connected to gluconeogenesis, glycolysis and citrate cycle as displayed in Figure 3. These results are consistent with those of

Gagaoua, Bonnet, & Picard (2020) who found that the energy metabolic enzymes MDH1, ENO3, ALDH1A1 and PGK1 were strongly correlated with WBSF values in bovine muscle. Therefore, our findings provide further support for the hypothesis that energy metabolism plays a key role in beef tenderness and related enzymes might be suitable biomarkers.

Immediately after slaughter, the oxygen supply is cut off and ATP is consumed. To compensate for the low amount of ATP, muscle glycogen is degraded and metabolized in anaerobic glycolysis preventing the formation of actomyosin cross-bridge. This also leads to the increase in the amount of lactate, H^+ and heat. Hence, the resulting metabolic acidosis can inhibit glycolytic enzymes, which affecting Ca^{+2} transport and binding capacity by actin-myosin interaction. The lack of ATP and Ca^{+2} in the sarcoplasm induces the formation of actomyosin cross-bridges causing *rigor mortis* (Huang, Larsen, Palmisano, Dai, & Lametsch, 2014). The sequence of these events explains the relationship between carbohydrates metabolism and beef tenderness. Additionally, the mitochondrial activity, particularly, the citrate cycle was altered to obtain ATP. In accordance with both metabolic pathways, other authors found increased amounts of enzymes associated with glycolytic and citrate cycle in early *post-mortem* as reviewed (Gagaoua, Terlouw, et al., 2020a). Even transcriptomic studies revealed data that supported the direct relationship between glycolysis/gluconeogenesis and the effect on the conversion of muscle to meat, suggesting that metabolic profile largely determines beef tenderness in early *post-mortem* (Bongiorni et al., 2016). Taking into account that these metabolic activities depend on fiber composition, more glycolytic fibers would provide more tender beef (Dang et al., 2020).

4. Conclusions

This study demonstrated that quantitative proteomics is an appealing approach to assess the protein changes during the process of tenderization. A total of 43 proteins were strongly associated with tenderness, therefore they could be proposed as protein biomarkers. Specifically, significant differential proteome changes of the two textural groups were associated with energy metabolism during early *post-mortem.* From the functional analysis, two clusters of proteins were identified as particularly relevant. The first cluster included the proteins ACO2, MDH1, MDH2 and CS and the second one comprised of FBP2, PFKL, LDHA, TPI1 and GAPDH/S, indicating that gluconeogenesis and specifically glycolysis and citrate cycle are key elements of beef tenderness. This research allowed us to deepen the knowledge on beef tenderness and its relationships with *post-mortem* biochemical events during the conversion of muscle into meat. Further studies are needed to validate these protein biomarkers and their role in beef tenderness. The findings of this study could have important implications in the meat industry for future applications.

Acknowledgments

Meat samples used in this study were obtained from the project "QUALIPIEM - Innovative tools for the selection of meat quality in the Piemontese breed", project number 2014/0249, funded by the Fondazione Cassa di Risparmio di Cuneo.

José M. Lorenzo and Daniel Franco belong to the competitive reference research group, FunMeat (Axencia Galega de Innovación, GAIN-IN607A2019/01) and they are members of the HealthyMeat network, funded by CYTED (Ref. 119RT0568)

Conflicts of Interest: The authors declare no conflict of interest.

References

Anderson, M. J., Lonergan, S. M., & Huff-Lonergan, E. (2012). Myosin light chain 1 release from myofibrillar fraction during postmortem aging is a potential indicator of proteolysis and tenderness of beef. *Meat Science*, *90*(2), 345–351. https://doi.org/10.1016/j.meatsci.2011.07.021

Anjo, S. I., Santa, C., & Manadas, B. (2017). SWATH-MS as a tool for biomarker discovery: From basic research to clinical applications. *Proteomics*, *17*(3–4). https://doi.org/10.1002/pmic.201600278

Antonelo, D., Gerrard, D. E., Gómez, J. F. M., Balieiro, J. C. C., Colnago, L. A., Beline, M., Cônsolo, N. R. B., Silva, S. L., Suman, S. P., Schilling, W., & Zhang, X. (2020). Metabolites and Metabolic Pathways Correlated With Beef Tenderness. *Meat and Muscle Biology*, *4*(1). https://doi.org/10.22175/mmb.10854

Arthur, P. (1995). Double muscling in cattle: a review. *Australian Journal of Agricultural Research*, *46*(8), 1493. https://doi.org/10.1071/ar9951493

Bhat, Z. F., Morton, J. D., Mason, S. L., & Bekhit, A. E. D. A. (2018). Role of calpain system in meat tenderness: A review. *Food Science and Human Wellness*, *7*(3), 196–204. https://doi.org/10.1016/j.fshw.2018.08.002

Biagini, D., & Lazzaroni, C. (2005). Carcass dissection and commercial meat yield in Piemontese and Belgian Blue double-muscled young bulls. *Livestock Production Science*, *98*(3), 199–204. https://doi.org/10.1016/j.livprodsci.2005.05.007

Bongiorni, S., Gruber, C. E. M., Chillemi, G., Bueno, S., Failla, S., Moioli, B.,

499 Ferrè, F., & Valentini, A. (2016). Skeletal muscle transcriptional profiles in
500 two Italian beef breeds, Chianina and Maremmana, reveal breed specific
501 variation. *Molecular Biology Reports*, *43*(4), 253–268.
502 https://doi.org/10.1007/s11033-016-3957-3

503 Boudon, S., Ounaissi, D., Viala, D., Monteils, V., Picard, B., & Cassar-Malek, I.
504 (2020). Label free shotgun proteomics for the identification of protein
505 biomarkers for beef tenderness in muscle and plasma of heifers. *Journal of*
506 *Proteomics*, *217*(January), 103685.
507 https://doi.org/10.1016/j.jprot.2020.103685

508 Boukha, A., Bonfatti, V., Cecchinato, A., Albera, A., Gallo, L., Carnier, P., &
509 Bittante, G. (2011). Genetic parameters of carcass and meat quality traits
510 of double muscled Piemontese cattle. *Meat Science*, *89*(1), 84–90.
511 https://doi.org/10.1016/j.meatsci.2011.03.024

512 Brugiapaglia, A., & Destefanis, G. (2011). *Colour variation during ageing in*
513 *Piemontese beef*. *57th Congress of Meat Science and Technology (pp. 1-*
514 *4)*, *7-12 August 2011*, *Ghent*, *Belgium.*, 7–9.

515 Brugiapaglia, A., Lussiana, C., & Destefanis, G. (2014). Fatty acid profile and
516 cholesterol content of beef at retail of Piemontese, Limousin and Friesian
517 breeds. *Meat Science*, *96*(1), 568–573.
518 https://doi.org/10.1016/j.meatsci.2013.08.012

519 Carlson, K. B., Prusa, K. J., Fedler, C. A., Steadham, E. M., Huff-Lonergan, E.,
520 & Lonergan, S. M. (2017). Proteomic features linked to tenderness of aged
521 pork loins. *Journal of Animal Science*, *95*(6), 2533–2546.
522 https://doi.org/10.2527/jas2016.1122

523 Chen, P. R., & Lee, K. (2016). Invited review: Inhibitors of myostatin as methods
524 of enhancing muscle growth and development. *Journal of Animal Science*,
525 *94*(8), 3125–3134. https://doi.org/10.2527/jas.2016-0532

526 Dang, D. S., Buhler, J. F., Thornton, K. J., Legako, J. F., & Matarneh, S. K.
527 (2020). Myosin heavy chain isoform and metabolic profile differ in beef
528 steaks varying in tenderness. *Meat Science*, *170*(June).
529 https://doi.org/10.1016/j.meatsci.2020.108266

530 Gagaoua, M., Bonnet, M., & Picard, B. (2020). Protein array-based approach to
531 evaluate biomarkers of beef tenderness and marbling in cows:
532 Understanding of the underlying mechanisms and prediction. *Foods*, *9*(9).
533 https://doi.org/10.3390/foods9091180

534 Gagaoua, M., Terlouw, E. M. C., Mullen, A. M., Franco, D., Warner, R. D.,
535 Lorenzo, J. M., Purslow, P., Gerrard, D., Hopkins, D. L., Troy, D., & Picard,
536 B. (2020a). Molecular signatures of beef tenderness: out-turns of research
537 and underlying mechanisms based on updated panel of protein biomarkers
538 from aggregated multi-platform proteomics datasets. *Meat Science*,
539 108311. https://doi.org/10.1016/j.meatsci.2020.108311

540 Gagaoua, M., Terlouw, E. M. C., Mullen, A. M., Franco, D., Warner, R. D.,
541 Lorenzo, J. M., Purslow, P. P., Gerrard, D., Hopkins, D. L., Troy, D., &
542 Picard, B. (2020b). Molecular signatures of beef tenderness: Underlying
543 mechanisms based on integromics of protein biomarkers from multi-
544 platform proteomics studies. *Meat Science*, *172*(September 2020), 108311.
545 https://doi.org/10.1016/j.meatsci.2020.108311

546 Henchion, M. M., McCarthy, M., & Resconi, V. C. (2017). Beef quality attributes:

547 A systematic review of consumer perspectives. *Meat Science*, *128*, 1–7.
548 https://doi.org/10.1016/j.meatsci.2017.01.006

549 Huang, C., Hou, C., Ijaz, M., Yan, T., Li, X., Li, Y., & Zhang, D. (2020).
550 Proteomics discovery of protein biomarkers linked to meat quality traits in
551 post- mortem muscles: Current trends and future prospects: A review.
552 *Trends in Food Science & Technology*, *40*(3), 82–85.
553 https://doi.org/10.4213/faa748

554 Huang, H., Larsen, M. R., Palmisano, G., Dai, J., & Lametsch, R. (2014).
555 Quantitative phosphoproteomic analysis of porcine muscle within 24h
556 postmortem. *Journal of Proteomics*, *106*, 125–139.
557 https://doi.org/10.1016/j.jprot.2014.04.020

558 Hughes, J. M., Clarke, F. M., Purslow, P. P., & Warner, R. D. (2020). Meat color
559 is determined not only by chromatic heme pigments but also by the
560 physical structure and achromatic light scattering properties of the muscle.
561 *Comprehensive Reviews in Food Science and Food Safety*, *19*(1), 44–63.
562 https://doi.org/10.1111/1541-4337.12509

563 Jia, X., Ekman, M., Grove, H., Færgestad, E. M., Aass, L., Hildrum, K. I., &
564 Hollung, K. (2007). Proteome changes in bovine longissimus thoracis
565 muscle during the early postmortem storage period. *Journal of Proteome*
566 *Research*, *6*(7), 2720–2731. https://doi.org/10.1021/pr070173o

567 Lana, A., & Zolla, L. (2016). Proteolysis in meat tenderization from the point of
568 view of each single protein: A proteomic perspective. *Journal of*
569 *Proteomics*, *147*, 85–97. https://doi.org/10.1016/j.jprot.2016.02.011

570 López-Pedrouso, M., Franco, D., Serrano, M. P., Maggiolino, A., Landete-

Castillejos, T., De Palo, P., & Lorenzo, J. M. (2019). A proteomic-based approach for the search of biomarkers in Iberian wild deer (Cervus elaphus) as indicators of meat quality. *Journal of Proteomics*, *205*(March), 103422. https://doi.org/10.1016/j.jprot.2019.103422

López-Pedrouso, M., Rodríguez-Vázquez, R., Purriños, L., Oliván, M., García-Torres, S., Sentandreu, M. Á., Lorenzo, J. M., Zapata, C., & Franco, D. (2020). Sensory and physicochemical analysis of meat from bovine breeds in different livestock production systems, pre-slaughter handling conditions, and ageing time. *Foods*, *9*(2), 1–17. https://doi.org/10.3390/foods9020176

Ludwig, C., Gillet, L., Rosenberger, G., Amon, S., Collins, B. C., & Aebersold, R. (2018). Data-independent acquisition-based SWATH - MS for quantitative proteomics: a tutorial . *Molecular Systems Biology*, *14*(8), 1–23. https://doi.org/10.15252/msb.20178126

Malheiros, J. M., Braga, C. P., Grove, R. A., Ribeiro, F. A., Calkins, C. R., Adamec, J., & Chardulo, L. A. L. (2019). Influence of oxidative damage to proteins on meat tenderness using a proteomics approach. *Meat Science*, *148*(July 2018), 64–71. https://doi.org/10.1016/j.meatsci.2018.08.016

Marino, R., Albenzio, M., della Malva, A., Santillo, A., Loizzo, P., & Sevi, A. (2013). Proteolytic pattern of myofibrillar protein and meat tenderness as affected by breed and aging time. *Meat Science*, *95*(2), 281–287. https://doi.org/10.1016/j.meatsci.2013.04.009

Moczkowska, M., Półtorak, A., & Wierzbicka, A. (2017). The effect of ageing on changes in myofibrillar protein in selected muscles in relation to the tenderness of meat obtained from cross-breed heifers. *International Journal*

595 *of Food Science and Technology*, *52*(6), 1375–1382.
596 https://doi.org/10.1111/ijfs.13436

597 Mwangi, F. W., Charmley, E., Gardiner, C. P., Malau-Aduli, B. S., Kinobe, R. T.,
598 & Malau-aduli, A. E. O. (2019). Diet and genetics influence beef cattle
599 performance and Meat Quality Characteristics. *Foods*, 1–24.

600 O'Quinn, T. G., Legako, J. F., Brooks, J. C., & Miller, M. F. (2018). Evaluation of
601 the contribution of tenderness, juiciness, and flavor to the overall consumer
602 beef eating experience. *Translational Animal Science*, *2*(1), 26–36.
603 https://doi.org/10.1093/tas/txx008

604 O'Rourke, B. A., Greenwood, P. L., Arthur, P. F., & Goddard, M. E. (2013).
605 Inferring the recent ancestry of myostatin alleles affecting muscle mass in
606 cattle. *Animal Genetics*, *44*(1), 86–90. https://doi.org/10.1111/j.1365-
607 2052.2012.02354.x

608 Ouali, A., Gagaoua, M., Boudida, Y., Becila, S., Boudjellal, A., Herrera-Mendez,
609 C. H., & Sentandreu, M. A. (2013). Biomarkers of meat tenderness:
610 Present knowledge and perspectives in regards to our current
611 understanding of the mechanisms involved. *Meat Science*, *95*(4), 854–870.
612 https://doi.org/10.1016/j.meatsci.2013.05.010

613 Pearce, K. L., Rosenvold, K., Andersen, H. J., & Hopkins, D. L. (2011). Water
614 distribution and mobility in meat during the conversion of muscle to meat
615 and ageing and the impacts on fresh meat quality attributes - A review.
616 *Meat Science*, *89*(2), 111–124.
617 https://doi.org/10.1016/j.meatsci.2011.04.007

618 Pegolo, S., Cecchinato, A., Savoia, S., Di Stasio, L., Pauciullo, A., Brugiapaglia,

619 A., Bittante, G., & Albera, A. (2020). Genome-wide association and
620 pathway analysis of carcass and meat quality traits in Piemontese young
621 bulls. *Animal*, *14*(2), 243–252. https://doi.org/10.1017/S1751731119001812

622 Picard, B., & Gagaoua, M. (2017). Proteomic Investigations of Beef
623 Tenderness. *Proteomics in Food Science: From Farm to Fork*, 177–197.
624 https://doi.org/10.1016/B978-0-12-804007-2.00011-4

625 Picard, B., & Gagaoua, M. (2020). Meta-proteomics for the discovery of protein
626 biomarkers of beef tenderness: An overview of integrated studies. *Food*
627 *Research International*, *127*(September 2019), 108739.
628 https://doi.org/10.1016/j.foodres.2019.108739

629 Savoia, S., Albera, A., Brugiapaglia, A., Di Stasio, L., Cecchinato, A., & Bittante,
630 G. (2019). Heritability and genetic correlations of carcass and meat quality
631 traits in Piemontese young bulls. *Meat Science*, *156*(May), 111–117.
632 https://doi.org/10.1016/j.meatsci.2019.05.024

633 Wu, W., Dai, R. T., & Bendixen, E. (2019). Comparing SRM and SWATH
634 Methods for Quantitation of Bovine Muscle Proteomes. *Journal of*
635 *Agricultural and Food Chemistry*, *67*(5), 1608–1618.
636 https://doi.org/10.1021/acs.jafc.8b05459

637 Zapata, I., Zerby, H. N., & Wick, M. (2009). Functional proteomic analysis
638 predicts beef tenderness and the tenderness differential. *Journal of*
639 *Agricultural and Food Chemistry*, *57*(11), 4956–4963.
640 https://doi.org/10.1021/jf900041j

641

CAPTIONS TO FIGURES

Figure 1. Heat map of differentially abundant proteins in *longissimus thoracis* of Piemontese young bulls. Protein intensities were $\log_{10}$ transformed and displayed in colors from green (high abundance) to red (low abundance). Both rows and columns are clustered using correlation distance and average linkage.

Figure 2. A) Functional enrichment analysis of differentially abundant proteins and correlated with and correlated with textural parameters in *ongissimus thoracis* of Piemontese young bulls using FunRich. The biological processes obtained were sorted by -log (p-value) and only top 6 are displayed; B) Protein-protein interaction network of differentially abundant proteins and correlated with and correlated with textural parameters in *ongissimus thoracis* of Piemontese young bulls using Search Tool for the Retrieval of Interacting Genes/proteins (STRING).

Figure 3. Summary of metabolic pathways for carbohydrates metabolism identified by proteomic analysis. The high and low abundance proteins were indicated by a green and red circle in tender and tough group, respectively. All reaction steps were obtained and adapted from KEGG (Kyoto Encyclopaedia of Genes and Genomes) pathways maps. https://www.kegg.jp/kegg/pathway.html

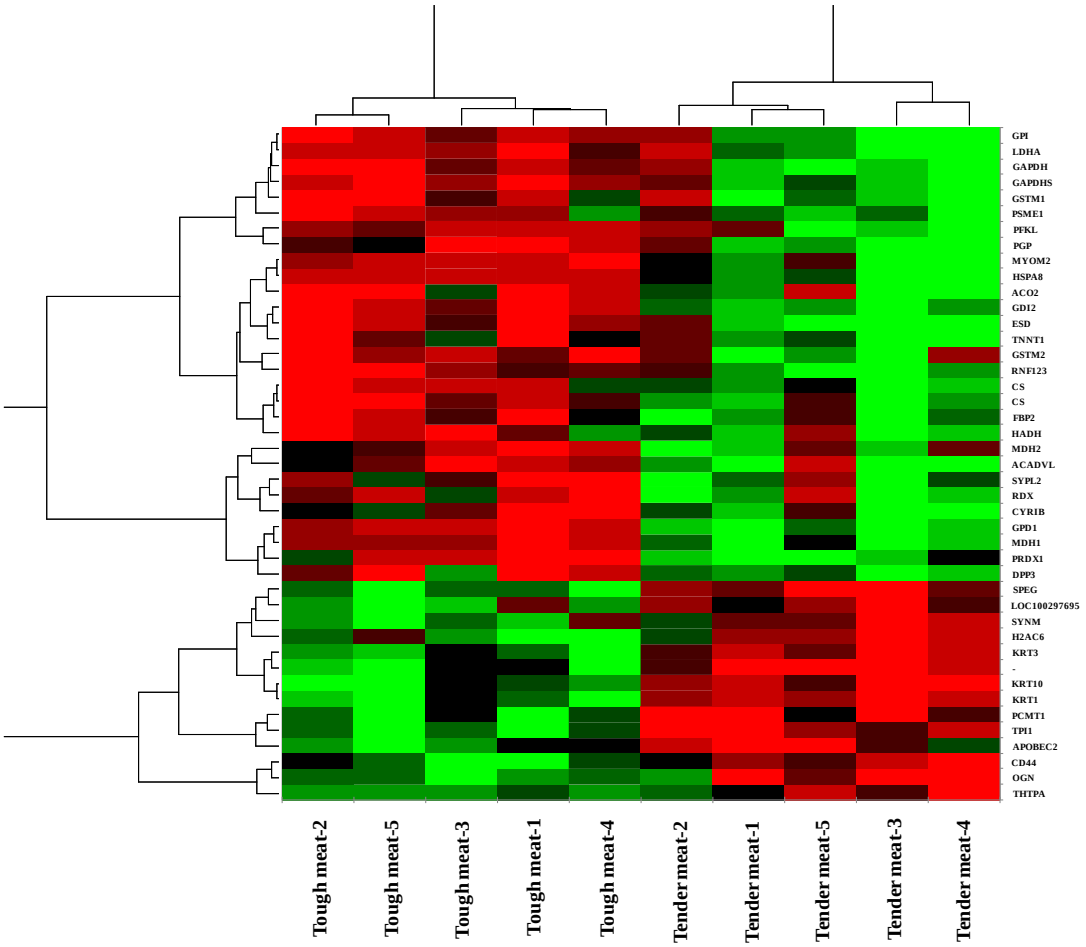
GPI
LDHA
GAPDH
GAPDHS
GSTM1
PSME1
PFKL
PGP
MYOM2
HSPA8
ACO2
GDI2
ESD
TNNT1
GSTM2
RNF123
CS
CS
FBP2
HADH
MDH2
ACADVL
SYPL2
RDX
CYRIB
GPD1
MDH1
PRDX1
DPP3
SPEG
LOC100297695
SYNM
H2AC6
KRT3
-
KRT10
KRT1
PCMT1
TPI1
APOBEC2
CD44
OGN
THTPA
Tough meat-2
Tough meat-5
Tough meat-3
Tough meat-1
Tough meat-4
Tender meat-2
Tender meat-1
Tender meat-5
Tender meat-3
Tender meat-4

Figure 1.

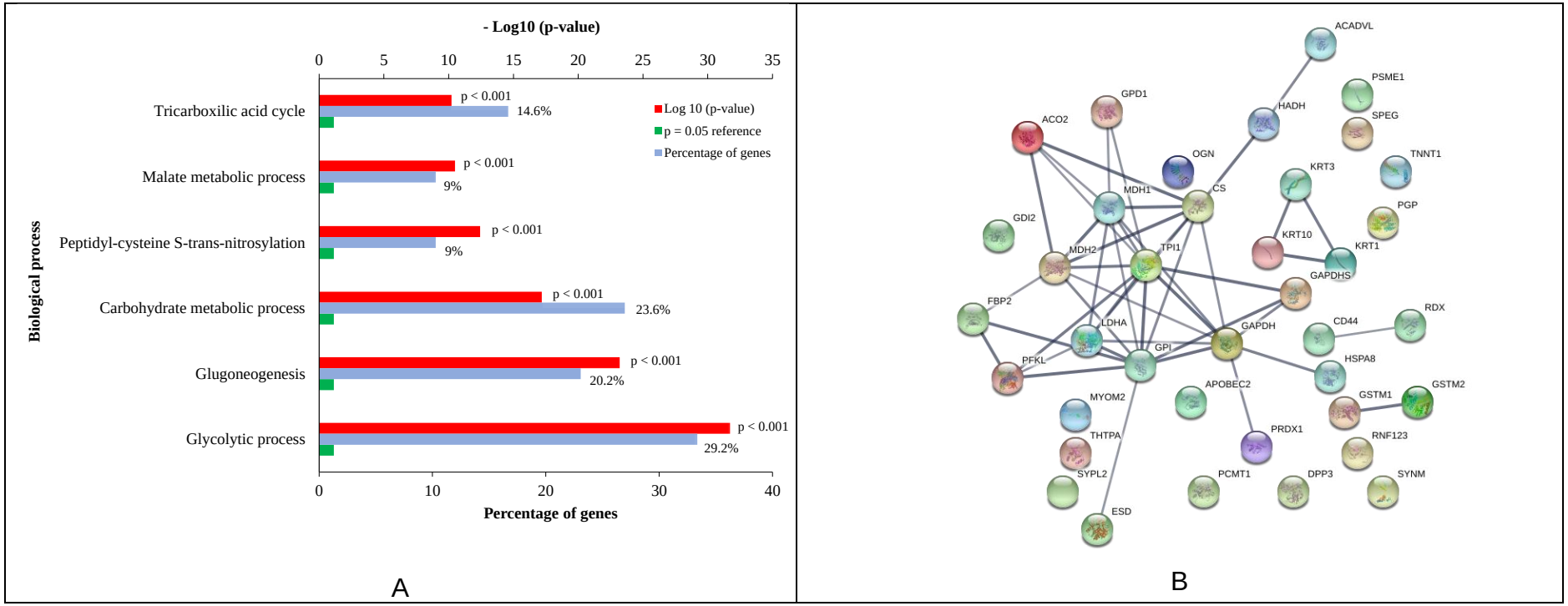
- Log10 (p-value)
0
5
10
15
20
25
30
35
Biological process
Tricarboxilic acid cycle
Malate metabolic process
Peptidyl-cysteine S-trans-nitrosylation
Carbohydrate metabolic process
Glugoneogenesis
Glycolytic process
p < 0.001
14.6%
p < 0.001
9%
p < 0.001
9%
p < 0.001
23.6%
p < 0.001
20.2%
p < 0.001
29.2%
Log 10 (p-value)
p = 0.05 reference
Percentage of genes
0
10
20
30
40
Percentage of genes
A
ACADVL
PSME1
GPD1
HADH
SPEG
ACO2
OGN
TNNT1
KRT3
MDH1
CS
PGP
GDI2
KRT10
KRT1
MDH2
TPI1
GAPDHS
FBP2
RDX
CD44
LDHA
GAPDH
GPI
HSPA8
PFKL
APOBEC2
GSTM2
GSTM1
MYOM2
PRDX1
THTPA
RNF123
SYPL2
PCMT1
DPP3
SYNM
ESD
B

Figure 2.

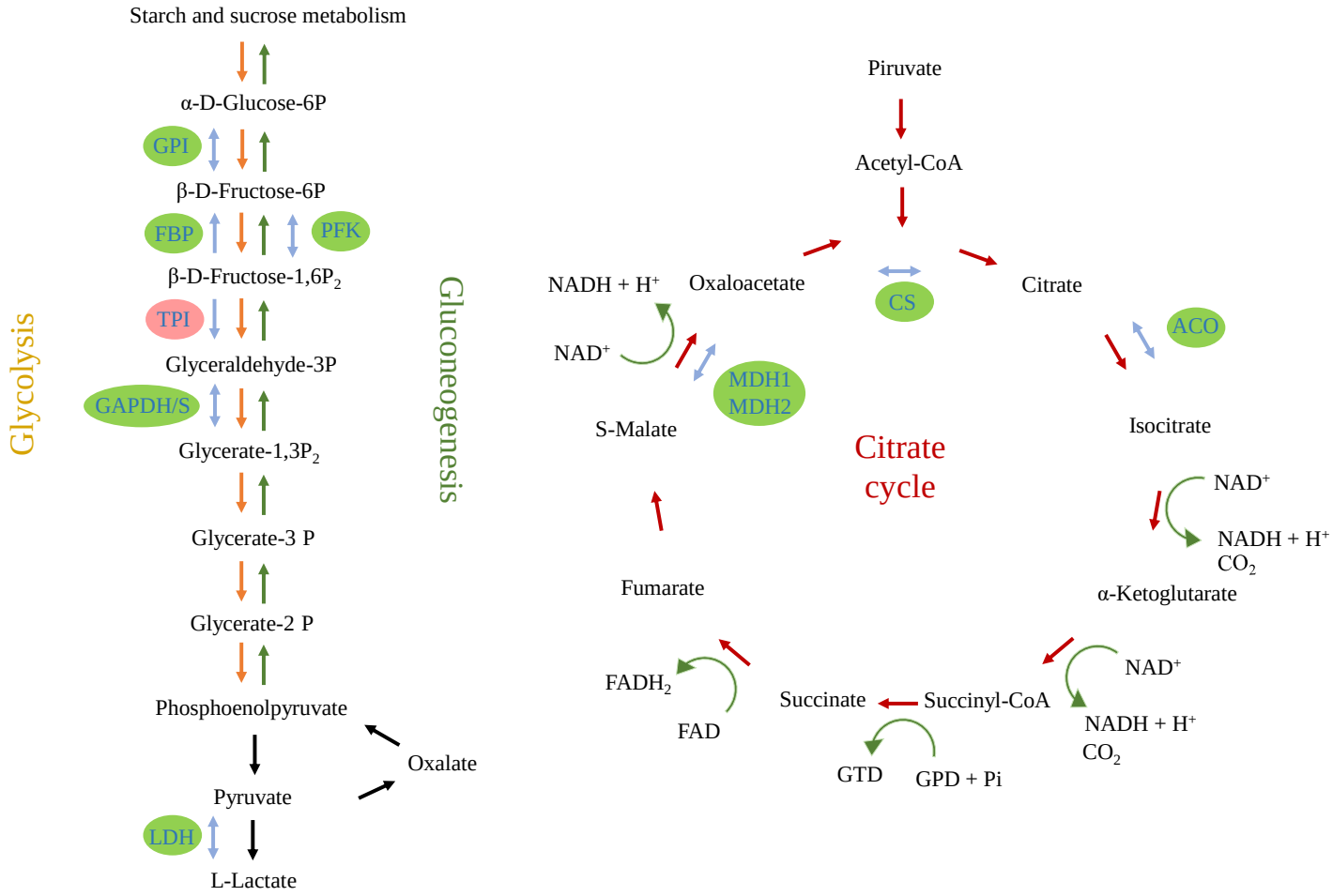

669

670 **Figure 3.**

671

672 **Table 1.** Meat quality parameters of aged meat from Piemontese young bulls (*longissimus thoracis*) for two textural groups: tender and tough.

	Tender	Tough	SEM	p-value
Chemical composition				
pH	5.53±0.04	5.56±0.03	0.01	0.266
Water (%)	74.89±0.32	74.78±0.92	0.20	0.816
Protein (%)	22.60±0.39	22.78±0.73	0.17	0.643
Fat (%)	0.92±0.19	1.15±0.40	0.01	0.297
Ash (%)	1.09±0.01	1.09±0.02	0.006	0.894
Collagen (%)	2.84±0.58	3.15±0.73	0.20	0.481
Soluble fraction (%)	10.91±1.47	6.96±1.21	0.77	0.002
Colour measurements				
Lightness (L*)	38.06±3.80	39.96±1.84	0.94	0.344
Redness (a*)	28.00±1.29	29.14±2.28	0.58	0.362
Yellowness (b*)	9.15±1.38	10.34±1.86	0.52	0.283
Chroma (C*)	29.47±1.64	30.93±2.78	0.72	0.340
Hue (h*)	18.02±1.89	19.41±1.83	0.60	0.270
MMb (%)	14.75±4.68	14.61±2.92	1.16	0.957
DMb (%)	12.27±5.10	11.70±5.36	1.56	0.870
OMb (%)	72.98±9.14	76.67±7.52	2.19	0.900
Water holding capacity				
Drip loss (%)	5.40±1.92	6.75±4.13	0.98	0.525
Cooking loss (%)	15.59±1.71	16.95±1.32	0.51	0.196
Textural parameters				
Shear force (N)	27.92±0.92	70.20±5.49	7.14	<0.001
Firmness (N/s)	6.47±1.20	16.37±2.41	1.74	<0.001
Energy (N)	110.34±22.81	320.31±198.15	54.70	0.046

673 MMb=Metmyoglobin; DMb=Deoxymyoglobin; OMb=Oxymyoglobin; Means ± SEM (standard error of mean)

674

675

676 **Table 2**. Quantification of differential abundant proteins (mean± SD) and fold change (*FC*) by SWATH obtained for two textural groups (tender
677 and though) in *longissimus thoracis* of Piemontese young bulls.

UniProt	Gene	Protein	Tough	Tender	*FC*	p-value
A0A3Q1LK65	THTPA	Thiamine-triphosphatase	14,713±400	9,279±1,887	1,59	0.023
A0A3Q1LMS5	HSPA8	Heat shock cognate 71 kDa protein	2,351,820±28,554	4,095,280±463,727	0,57	0.006
A0A3Q1LQ76	ACADVL	Very long-chain-specific acyl-CoA dehydrogenase	1,054±254	3,817±849	0,28	0.014
A0A3Q1LTB0	MDH2	Malate dehydrogenase	697,210±66,648	1,075,476±149,847	0,65	0.049
A0A3Q1LY19	LDHA	L-lactate dehydrogenase	7,249,000±618,311	14,295,620±2,532,085	0,51	0.027
A0A3Q1M430	TNNT1	Troponin T, slow skeletal muscle	256,492±42,701	471,824±70,816	0,54	0.032
A0A3Q1M6K7	PFKL	ATP-dependent 6-phosphofructokinase	586,566±16,698	900,780±121,087	0,65	0.033
A0A3Q1M8J9	GAPDH	Glyceraldehyde-3-phosphate dehydrogenase	33,267,200±2,443,100	58,623,800±6,348,046	0,57	0.006
A0A3Q1MAU7	ESD	S-formylglutathione hydrolase	106,745±8,285	179,568±15,974	0,59	0.004
A0A3Q1MK34	FBP2	Fructose-1,6-bisphosphatase isozyme 2	744,886±69,514	1,166,928±94,395	0,64	0.007
A0A3Q1MP70	GPI	Glucose-6-phosphate isomerase	7,766,760±471,343	13,899,540±1,742,447	0,56	0.009
A0A3Q1N7H1	CYRIB	Protein FAM49B	7,830±2,311	22,203±4,177	0,35	0.017
A0A452DI24	GDI2	Rab GDP dissociation inhibitor	51,049±2,738	83,760±5,864	0,61	0.001
A0A452DIW4	MDH1	Malate dehydrogenase	2,555,140±259,281	4,766,100±464,963	0,54	0.003
A0A452DIX3	TPI1	Triosephosphate isomerase	99,101,200±8,864,196	59,412,800±4,310,739	1,67	0.004
A0A452DJ69	APOBEC2	C->U-editing enzyme APOBEC-2	1,383,250±229,200	766,522±121,159	1,80	0.045
A0A452DJJ3	GPD1	Glycerol-3-phosphate dehydrogenase	2,197,600±130,598	3,624,520±123,598	0,61	<0.001

A4IFG0	GSTM1	GSTM1 protein	269,456±38,103	459,626±59,230	0,59	0.027
A5PKM0	GSTM2	GSTM2 protein (Fragment)	24,768±1,200	42,594±7,088	0,58	0.038
A6QNZ7	KRT10	Keratin 10	349,726±39,132	203,382±17,331	1,72	0.009
E1BF23	MYOM2	Myomesin 2	759,554±17,052	1,238,776±145,850	0,61	0.012
E1BIS6	SYNM	Synemin	104,115±10,072	66,665±8,157	1,56	0.020
E1BL26	RNF123	Ring finger protein 123	71,082±12,558	191,703±36,365	0,37	0.014
F1MJJ8	RDX	Radixin	95,758±9,888	148,769±16,765	0,64	0.026
F2Z4J1	H2AC6	Histone H2A	27,888±3,952	12,563±2,477	2,22	0.011
G3MXL3	KRT3	Keratin 3	452,456±50,826	264,852±22,803	1,71	0.010
G3MZZ6	PCMT1	Protein-L-isoaspartate O-methyltransferase	732,408±70,772	460,204±48,354	1,59	0.013
G3N022	SPEG	Striated muscle enriched protein kinase	66,760±3,497	43,744±3,276	1,53	0.001
G3N0V2	KRT1	Keratin 1	738,836±73,777	412,236±23,890	1,79	0.003
M0QVY0	-	Uncharacterized protein	203,612±17,116	127,970±8,151	1,59	0.004
M5FJY9	PGP	Phosphoglycolate phosphatase	99,050±11,004	168,750±16,810	0,59	0.009
O77679	GAPDHS	Glyceraldehyde 3-phosphate dehydrogenase (Fragment)	3,752,100±203,915	6,722,280±901,058	0,56	0.012
Q0QEK4	CS	Citrate synthase (Fragment)	199,920±30,144	476,716±74,611	0,42	0.009
Q0VBZ3	SYPL2	Synaptophysin-like 2	53,039±6,354	8,2642±10,758	0,64	0.046
Q0VD03	CD44	CD44 antigen	14,708±1,643	8,329±1,242	1,77	0.015
Q1P9Q3	ACO2	Aconitate hydratase, (Fragment)	16,140±2,844	37,859±8,529	0,43	0.042
Q2KJC5	HADH	Hydroxyacyl-Coenzyme A dehydrogenase	73,550±9,423	112,301±11,241	0,65	0.030

Q2KJE7	PSME1	Proteasome (Prosome, macropain) activator subunit 1	71,930±10,333	109,920±10,682	0,65	0.034
Q3T085	OGN	OGN protein	386,988±33,992	239,476±36,748	1,62	0.019
Q58CS3	DPP3	Dipeptidyl peptidase 3	29,896±5,326	48,232±3,079	0,62	0.018
Q8WMY1	CS	Citrate synthase (Fragment)	65,862±9,523	132,440±20,471	0,50	0.019
Q9BGI4	PRDX1	Peroxiredoxin 1	710,542±68,049	1,122,282±60,571	0,63	0.002
V6F869	LOC100297695	Apolipoprotein A-I-like	38,157±6,022	17,751±3,541	2,15	0.019

678

679